



## OPEN Broadly reactive monoclonal antibodies against beta-lactamases for immunodetection of bacterial resistance to antibiotics

Karolina Bielské<sup>1✉</sup>, Rasa Petraitytė-Burneikienė<sup>1</sup>, Aliona Avižinienė<sup>1</sup>, Justas Dapkūnas<sup>1</sup>, Ieva Plikusienė<sup>2</sup>, Silvija Juciutė<sup>2</sup>, Miglė Stančiauskaitė<sup>2</sup>, Aurelija Žvirblienė<sup>1</sup> & Indrė Kučinskaitė-Kodžė<sup>1</sup>

With antibiotic resistance reaching alarming levels globally, rapid detection of resistance determinants is crucial for administering appropriate antimicrobial therapies. This study aimed to develop monoclonal antibodies (MAbs) against bacterial  $\beta$ -lactamases, which are key enzymes in antibiotic resistance, for potential diagnostic use. To generate MAbs capable of recognising a broad range of  $\beta$ -lactamases in bacterial isolates, the bacteriophage vB\_EcoS\_NBD2 tail tube protein gp39-derived nanotubes, as a scaffold displaying a highly conserved 17-amino acid peptide of AmpC  $\beta$ -lactamases, were produced in yeast and used as an immunogen for generation of MAbs by hybridoma technology. Thirteen hybridoma clones producing peptide-specific MAbs were developed. To assess MAb reactivity with AmpC enzymes, recombinant DHA-1, PDC-195, ACT-14, CMY-34, and ADC-144  $\beta$ -lactamases were generated. Eleven of thirteen MAbs demonstrated cross-reactivity with all tested  $\beta$ -lactamases in ELISA and Western blot. Immunoprecipitation and Western blot analyses confirmed MAb reactivity with natural CMY-34 in the *Citrobacter portucalensis* isolate. Epitope analysis revealed that most MAbs recognise a highly conserved epitope of 11 amino acids. The MAbs were comprehensively characterised using different immunoassays, total internal reflection ellipsometry and computational modelling. These novel MAbs, which recognise a wide range of AmpC enzymes, represent a promising tool for immunodetection of antibiotic resistance determinants.

**Keywords** AmpC  $\beta$ -lactamases, Class C  $\beta$ -lactamases,  $\beta$ -lactamase detection, Monoclonal antibodies, Antibiotic resistance

Increasing levels of resistance to antibiotics in bacteria are among the greatest threats to human health in this century<sup>1</sup>. Among various antimicrobial resistance mechanisms, the action of  $\beta$ -lactamases is the most prevalent. These enzymes enable bacteria to neutralise  $\beta$ -lactam antibiotics, which are crucial in the treatment of bacterial infections. By breaking the  $\beta$ -lactam ring structure,  $\beta$ -lactamases render these antibiotics ineffective. Based on their structure and mechanism of action,  $\beta$ -lactamases are classified into four groups: A, B, C, and D. Class A, C, and D enzymes hydrolyse  $\beta$ -lactams utilising serine, and class B enzymes contain zinc ions in their active site<sup>2</sup>. Class C  $\beta$ -lactamases, also termed AmpC  $\beta$ -lactamases, are among the most common and clinically significant resistance determinants<sup>3,4</sup>. Based on amino acid sequence homology, class C consists of 32 families of  $\beta$ -lactamases (DHA, CMY, ADC, PDC, ACT, FOX, LAT, etc.). These families are composed of high variety of  $\beta$ -lactamase allelic variants comprising more than 46% of all identified  $\beta$ -lactamases described in the Beta-Lactamase DataBase (BLDB) (last updated: January 4, 2025; <http://www.bldb.eu/>)<sup>5</sup>. According to phylogenetic analysis, these enzymes are highly heterogeneous and contain hundreds of clinically relevant variants, which cannot be identified by one universal assay<sup>6</sup>. AmpC  $\beta$ -lactamases are typically chromosomally encoded and can be expressed in certain bacteria. They are mostly identified in extended-spectrum cephalosporin-resistant gram-negative bacteria, predominantly in *Enterobacteriaceae* species<sup>4</sup>. In some of them, such as *Citrobacter freundii*, *Enterobacter* spp., *Serratia marcescens* or *Pseudomonas aeruginosa*, AmpC is encoded by inducible chromosomal genes. In contrast, non-inducible chromosomal resistance is observed in *Escherichia coli*, *Acinetobacter*

<sup>1</sup>Institute of Biotechnology, Life Sciences Center, Vilnius University, Saulėtekio av. 7, Vilnius LT-10257, Lithuania.

<sup>2</sup>Faculty of Chemistry and Geosciences, Institute of Chemistry, Vilnius University, Naugarduko g. 24, Vilnius LT-03225, Lithuania. ✉email: karolina.bielske@gmc.vu.lt

*baumannii* and *Shigella* species. Plasmid-mediated AmpC  $\beta$ -lactamases have been identified in *Salmonella enterica*, *E. coli*, *Proteus mirabilis*, *Klebsiella pneumoniae* and *K. oxytoca*<sup>7,8</sup>. Plasmid-encoded AmpC genes carry the threat of spreading among organisms within hospitals or between different geographical regions<sup>4</sup> as these enzymes mediate resistance to most penicillins, broad-spectrum cephalosporins, cephamycins and major  $\beta$ -lactamase inhibitor- $\beta$ -lactam combinations<sup>4,9</sup>.

AmpC-producing gram-negative bacteria represent a significant challenge in the management of infectious diseases. These antibiotic-resistant organisms can cause a variety of community- and hospital-acquired infections, such as pneumonia, urinary tract, bloodstream and surgical-site infections. They are also associated with central nervous system diseases, such as meningitis<sup>10</sup>. The choice of antibiotics for treatment and monitoring of bacterial susceptibility varies across healthcare settings. Additionally, differences in the prevalence of infectious diseases contribute to variations in antibiotic resistance mechanisms among different geographical regions. Therefore, epidemiological surveillance is critically important for comprehensively evaluating and monitoring the extent of the antibiotic resistance profile in pathogens for effective interventions. Accurate epidemiological data is essential for establishing appropriate treatment recommendations and implementing national or local antibiotic use<sup>11,12</sup>. For example, the ESCPM group of bacteria (*Enterobacter* species, such as *K. aerogenes*, *Serratia* sp., *C. freundii* complex, *Providencia* sp. and *Morganella morganii*) carrying chromosomal AmpC  $\beta$ -lactamases has not yet been included in systemic antimicrobial resistance surveillance programs<sup>13,14</sup>. An observational study of ESCPM species isolated from blood cultures in 27 European hospitals over the period of 2020–2022 demonstrated that AmpC overproduction was the most prevalent (15.8%) resistance mechanism in the tested bacterial isolates. Furthermore, the study revealed that only 29.6% of the analysed hospitals routinely tested and characterised the AmpC profile and production mechanisms in ESCPM isolates<sup>13</sup>.

MAbs specific to  $\beta$ -lactamases can be applied for AmpC detection in bacterial isolates and serve as useful molecular tools in epidemiological studies and profiling of resistance mechanisms. However, no such antibodies capable of detecting a broad variety of AmpC enzymes have been described yet. In this study, we describe novel, broadly reactive and comprehensively characterised MAbs raised against a conserved sequence of AmpC  $\beta$ -lactamases. For MAb generation, an efficient chimeric immunogen, based on bacteriophage-derived nanotubes displaying a selected conserved sequence of AmpC  $\beta$ -lactamases, was utilised. Previous studies demonstrated that bacteriophage-derived nanotubes mimic the structure of native virus and can be engineered by incorporating foreign protein fragments, transforming them into immunogenic tools for antigen presentation<sup>15,16</sup>. These nanotubes can be used as an alternative to traditional immunogenicity enhancing protein carriers, such as tetanus toxoid (TT), diphtheria toxoid (DT), genetically modified nontoxic variant of diphtheria toxin (CRM197), meningococcal outer membrane protein complex (OMPC), *Haemophilus influenzae* protein D or keyhole limpet hemocyanin (KLH)<sup>17,18</sup>.

## Results

### Production and characterisation of the recombinant chimeric immunogen

In the first step, we aimed to identify a universal sequence within AmpC  $\beta$ -lactamases and use it as an antigenic epitope to develop hybridomas that secrete broadly-reactive MAbs capable of detecting a wide range of AmpC  $\beta$ -lactamases. To achieve this goal, a universal epitope sequence was identified through the alignment of  $\beta$ -lactamase amino acid (aa) sequences corresponding to currently identified families of class C  $\beta$ -lactamases in the Beta-Lactamase DataBase (BLDB) (last updated: January 4, 2025; <http://www.bldb.eu/>)<sup>5</sup>. The alignment revealed a conserved 17 aa-long region (Fig. 1a; Supplementary information file 1). On the basis of these findings, the sequence corresponding to aa residues 77–93 of the DHA-1  $\beta$ -lactamase (GenBank no. AEP68014.1) was selected as the reference sequence and referred to as DHA-1<sub>77–93</sub>. For immunogen construction, previously described<sup>15</sup> chimeric polytubes formed by the tail tube protein gp39 of bacteriophage vB\_EcoS\_NBD2, spanning aa residues 6–238, were selected as an epitope-displaying scaffold (gp39m). To minimise any potential impact of the inserted DHA-1<sub>77–93</sub> fragment on gp39 self-assembly, a chimeric protein variant, gp39m\_linker\_DHA, with an introduced linker between the scaffold protein gp39m and the DHA-1<sub>77–93</sub> insert was employed (Fig. 1b; Supplementary information file 2, Fig. S1).

The synthesis of the chimeric gp39m\_linker\_DHA protein was carried out in the *Saccharomyces cerevisiae* strain AH22-214, and the polytubes formed by chimeric protein was concentrated by ultracentrifugation on a sucrose gradient. Sodium dodecyl sulphate polyacrylamide gel electrophoresis (SDS-PAGE) revealed that the synthesis efficiency of gp39m\_linker\_DHA in yeast was similar to that of unmodified gp39 (Fig. 1c, yellow arrows). To assess self-assembly properties of the gp39m\_linker\_DHA protein, transmission electron microscopy (TEM) was employed. The analysis confirmed that the insertion of the DHA-1<sub>77–93</sub> fragment at the C-terminus of the gp39m\_linker protein was well tolerated and was in line with our previous findings<sup>15</sup>. Thus, the chimeric protein self-assembled into well-ordered and flexible polytubes, displaying a morphology similar to that of unmodified gp39, with a width of 12–14 nm and length ranging from 0.1 to over 1  $\mu$ m (Fig. 1d).

### Generation and characterisation of MAbs against the DHA-1<sub>77–93</sub> sequence

For generation of MAbs, mice were immunised with the chimeric protein gp39m\_linker\_DHA. In total, 13 hybridoma clones producing DHA-1<sub>77–93</sub>-specific IgG MAbs were isolated and further characterised using various immunoassays (Table 1). Most of the MAbs were of the IgG3 subclass. For specificity testing, several members of different AmpC families, identified in various species of gram-negative bacteria, were selected. For analysis, recombinant DHA-1 (rDHA-1), PDC-195 (rPDC-195), ACT-14 (rACT-14), CMY-34 (rCMY-34) and maltose binding protein (MBP)-fused AmpC  $\beta$ -lactamase ADC-144 (rMBP-ADC-144) were synthesised in *E. coli* and purified by affinity chromatography. The purified  $\beta$ -lactamases were further characterised for their enzymatic activity by the cefinase test (Supplementary information file 2, Fig. S4). All recombinant proteins were

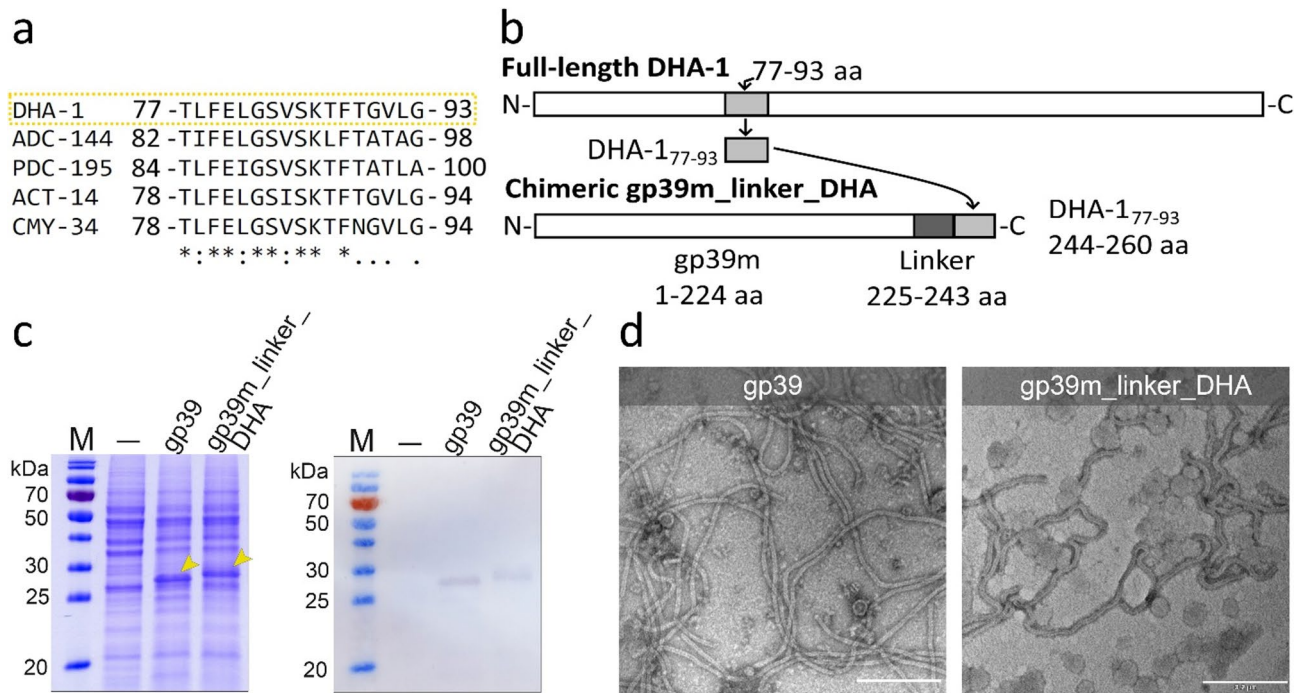


**Fig. 1.** Production and analysis of the chimeric gp39m\_linker\_DHA protein. **(a)** Alignment of the conserved aa region of DHA-1 (GenBank no. AEP68014.1) (squared in yellow), CMY-34 (GenBank no. ABN51006.1), ACT-14 (GenBank no. AFU25647.1), PDC-195 (GenBank no. AHH52937.1) and ADC-144 (GenBank no. OVK75103.1)  $\beta$ -lactamases. An asterisk “\*” denotes positions that have a single, fully conserved residue. A period “.” indicates conservation between groups of weakly similar properties. A colon “:” indicates conservation between groups of strongly similar properties. **(b)** Schematic representation of chimeric protein construction. A 77–93 aa region of DHA-1 (DHA-1<sub>77–93</sub>) was fused with the tail tube protein gp39 of the bacteriophage, introducing a linker sequence (indicated in Supplementary information file 2, Fig. S1). **(c)** SDS-PAGE and WB analysis of yeast-expressed gp39 protein variants (indicated by yellow arrows). The lysates of yeast expressing gp39 and gp39m\_linker\_DHA were analysed. The dash “-” indicates the lysate of yeast transformed with the vector pFX7 without the DHA-1<sub>77–93</sub> coding sequence. For WB analysis, gp39 protein-specific in-house generated mouse polyclonal antibodies<sup>16</sup> were used. M – molecular weight marker Page Ruler Prestained protein ladder (Thermo Scientific, 26616). The original blot and gel data are presented in Supplementary information file 2, Fig. S2. **(d)** Electron micrographs of chimeric nanotubes. The scale bars represent 200 nm. The original micrographs are presented in Supplementary information file 2, Fig. S3.

confirmed to be enzymatically active, indicating their proper folding and remaining functional activity during purification.

The reactivity of generated MAbs with different recombinant  $\beta$ -lactamases was confirmed by indirect enzyme-linked immunosorbent assay (ELISA) and Western blot (WB) (Table 1; Fig. 2a, which represents examples of MAb reactivity; Supplementary information file 2, Fig. S5). All tested MAbs, except 24F1 and 15F2, were able to recognise the rDHA-1, rPDC-195, rACT-14, rCMY-34 and rMBP-ADC-144 proteins in both immunoassays, whereas MAbs 24F1 and 15F2 recognised rDHA-1, rACT-14 and rCMY-34 but did not react with rPDC-195 or rMBP-ADC-144. No MAb reactivity was observed with irrelevant proteins used as negative controls, including gp39m\_linker, MBP, yeast lysate or recombinant class B  $\beta$ -lactamase NDM-1 (rNDM-1).

Additionally, MAb affinity to recombinant  $\beta$ -lactamases was evaluated by determining the apparent affinity values using indirect ELISA. The values for MAb binding to rDHA-1 ranged from 0.05 to 0.4 nM, demonstrating high apparent affinity to the antigen. Obtained apparent affinity values for highly cross-reactive MAbs (excluding MAbs 24F1 and 15F2) with other tested recombinant  $\beta$ -lactamases ranged from 0.04 to 1 nM, indicating high apparent affinity to homologous AmpC  $\beta$ -lactamases (Table 1).

The ability of MAbs raised against the DHA-1<sub>77–93</sub> sequence to recognise natural  $\beta$ -lactamases was tested using a previously described<sup>19</sup> CMY-34-producing *C. portucalensis* isolate (3826Z08). For this purpose, a lysate of *C. portucalensis* was prepared with determined total protein concentration, and the retained enzymatic activity of CMY-34 was confirmed by cefinase test (Supplementary information file 2, Fig. S4). All generated MAbs efficiently detected natural CMY-34 in the *C. portucalensis* lysate in WB (Fig. 2b, which represents examples of MAb reactivity; Supplementary information file 2, Fig. S7).

MAb reactivity with rDHA-1 and natural CMY-34 was additionally confirmed by immunoprecipitation (IP) (Fig. 2c, which represents examples of MAb reactivity; Supplementary information file 2, Fig. S9). Natural CMY-34 was isolated from *C. portucalensis* lysate using MAbs against DHA-1<sub>77–93</sub> coupled with rProtein G Sepharose (Cytiva, 17127905). Using this method, a 35 kDa protein corresponding to CMY-34 was successfully

No.	MAb clone	Isotype	Assay <sup>a</sup>	MAB reactivity with recombinant $\beta$ -lactamases				
				rDHA-1	rPDC-195	rACT-14	rCMY-34	rMBP-ADC-144
1.	21C12	IgG3	ELISA	0.4	0.2	0.5	0.2	1.1
			WB	+	+	+	+	+
2.	24F1	IgG3	ELISA	0.3	60.5	0.3	0.2	–
			WB	+	–	+	+	–
3.	15F7	IgG1	ELISA	0.07	0.1	0.2	0.05	0.3
			WB	+	+	+	+	+
4.	3B9	IgG2a	ELISA	0.06	0.05	0.1	0.04	0.2
			WB	+	+	+	+	+
5.	25C2	IgG3	ELISA	0.4	0.3	0.4	0.1	0.9
			WB	+	+	+	+	+
6.	26C9	IgG1	ELISA	0.08	0.2	0.4	0.9	0.4
			WB	+	+	+	+	+
7.	13F9	IgG3	ELISA	0.3	0.3	0.4	0.2	0.8
			WB	+	+	+	+	+
8.	15F2	IgG3	ELISA	0.2	9.1	0.4	0.2	–
			WB	+	–	+	+	–
9.	16E6	IgG3	ELISA	0.2	0.2	0.4	0.2	0.7
			WB	+	+	+	+	+
10.	6A7	IgG3	ELISA	0.3	0.2	0.4	0.2	0.6
			WB	+	+	+	+	+
11.	5G8	IgG3	ELISA	0.4	0.3	0.5	0.2	0.9
			WB	+	+	+	+	+
12.	5C12	IgG2a	ELISA	0.05	0.07	0.1	0.03	0.2
			WB	+	+	+	+	+
13.	3B12	IgG3	ELISA	0.3	0.05	0.5	0.2	0.7
			WB	+	+	+	+	+

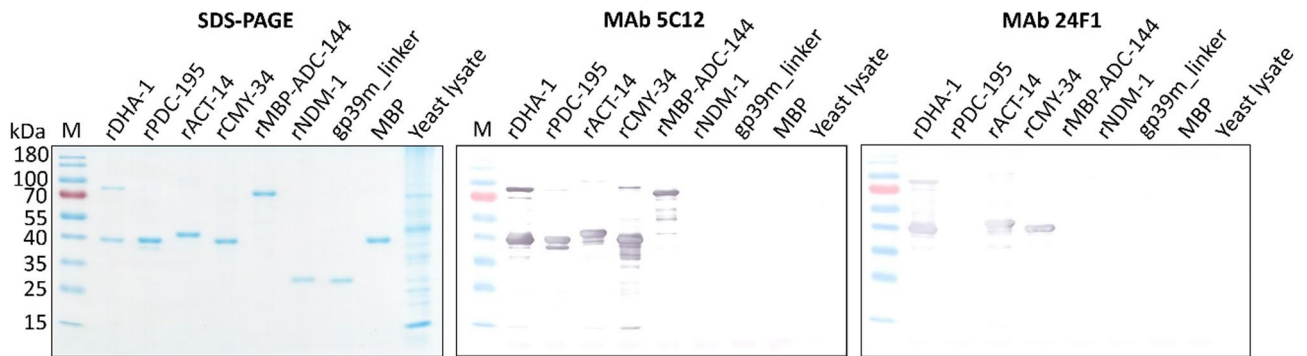
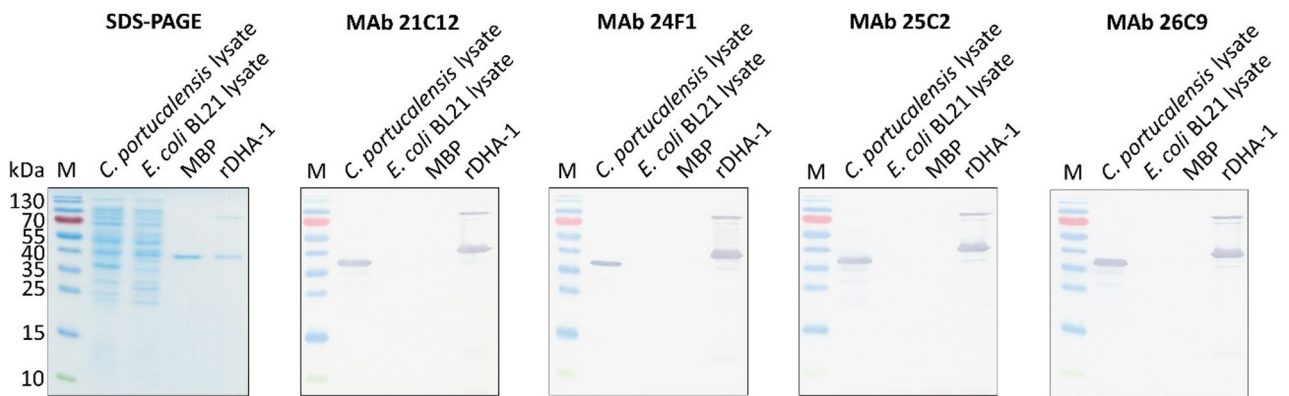
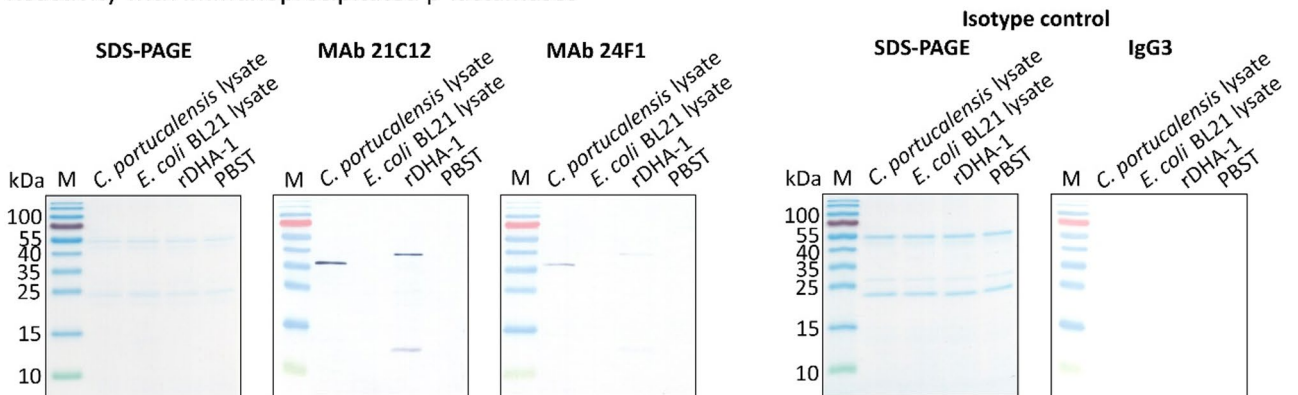
**Table 1.** Characterisation of MABs generated against the chimeric gp39m\_linker\_DHA protein. <sup>a</sup>ELISA results are presented as apparent affinity values, which represent MAb concentration (nM) required to achieve 50% of the maximum binding to the respective antigen; “–” indicates a negative result in ELISA; in WB the visible band was defined as a positive result (+), and the absence of the visible band was defined as a negative result (–).

immunoprecipitated from the bacterial lysate with MABs 21C12, 24F1 and 15F2, demonstrating their reactivity with natural  $\beta$ -lactamase (Fig. 2c; Supplementary information file 2, Fig. S9).

### Fine mapping of MAB epitopes

To specify the MAB recognition sites (epitopes) within DHA-1<sub>77–93</sub>, MABs were tested with overlapping synthetic peptides (P0–P8) spanning the conserved 17 aa-long sequence (77–83 aa region) of DHA-1 by ELISA (Fig. 3a; Table 2). The analysis identified two distinct interaction sites of the MABs within DHA-1<sub>77–93</sub>. One group of MABs, designated as Group 1, was reactive with P0–P2 and P5–P7 peptides (Table 2; Fig. 3a). These MABs recognised an 11 aa-long epitope (Table 2; Fig. 3b) localised within a 79–89 aa region of DHA-1 (Fig. 3c). In contrast, MABs 24F1 and 15F2 were able to recognise P0–P5 peptides, which encompass a 9 aa-long epitope within an 85–93 aa region of DHA-1, therefore, these MABs were assigned to Group 2 (Table 2; Fig. 3a, b, c).

After the aa sequence of DHA-1<sub>77–93</sub> was aligned with those of the ACT-14, PDC-195, CMY-34 and ADC-144  $\beta$ -lactamases used for MAB characterisation, sequence heterogeneity was observed at the C-terminus of the compared regions (Fig. 3d). Specifically, PDC-195 displayed 3 aa differences at the C-terminus in an 84–100 aa region, whereas compared with DHA-1<sub>77–93</sub>, ADC-144 showed 4 aa mismatches in the 82–98 aa segment. These aa alterations likely explain the weak reactivity of the MABs 24F1 and 15F2, which target the epitope localised at the C-terminus of the homologous fragment within the rPDC-195 and rMBP-ADC-144 proteins. In contrast, the epitope of Group 1 MABs exhibited high similarity among the aa sequences of ACT-14, PDC-195, CMY-34 and ADC-144 (Fig. 3d). To evaluate a potential broad-reactivity of the MABs, the recognition site of Group 1 MABs was further compared with a wide range of AmpC  $\beta$ -lactamases. Due to a narrower reactivity with AmpC enzymes, Group 2 MABs were excluded from the further analysis. The sequence alignment of Group 1 epitope revealed that a 79–89 aa region of DHA-1 is highly conserved among DHA family members and 14 other families of AmpC  $\beta$ -lactamases (Fig. 3e). Families, such as PDC, clustered with six other  $\beta$ -lactamase families, ACT with one family and CMY with two families on the basis of sequence similarity (Fig. 3e), suggesting potential broad-reactivity of the antibodies. To further confirm MAB reactivity with other members of AmpC  $\beta$ -lactamases, an

**a**Reactivity with recombinant  $\beta$ -lactamases**b**Reactivity with natural CMY-34  $\beta$ -lactamase**c**Reactivity with immunoprecipitated  $\beta$ -lactamases

**Fig. 2.** Representative reactivity patterns of the MAbs raised against the DHA-1<sub>77–93</sub> sequence with different  $\beta$ -lactamases. **(a)** MAb reactivity with recombinant  $\beta$ -lactamases in WB. Irrelevant rNDM-1  $\beta$ -lactamase, gp39m\_linker, maltose binding protein (MBP) and yeast lysate were used as negative controls. Original blots and gels are presented in Supplementary information file 2, Fig. S6. **(b)** MAb reactivity with the natural CMY-34  $\beta$ -lactamase in *C. portucalensis* lysate tested by WB. *E. coli* BL21 lysate and MBP were used as negative controls. Original blots and gels are presented in Supplementary information file 2, Fig. S8. **(c)** Immunoprecipitation of rDHA-1 and natural CMY-34. *C. portucalensis* lysate was used as a source of natural CMY-34. *E. coli* BL21 lysate and protein dilution buffer (PBST) were used as negative controls. In-house produced irrelevant IgG3 MAb 20D1 against the SARS-CoV-2 spike protein was tested as an isotype control. The WB result was developed using horseradish peroxidase-conjugated MAb 26C9 against DHA-1<sub>77–93</sub>. SDS-PAGE of immunoprecipitated proteins with MAbs 24F1, 21C12 and the isotype control are shown. Images of the original blots and gels are presented in Supplementary information file 2, Fig. S10. M – molecular weight marker PageRuler Prestained Protein Ladder (Thermo Scientific, 26616).

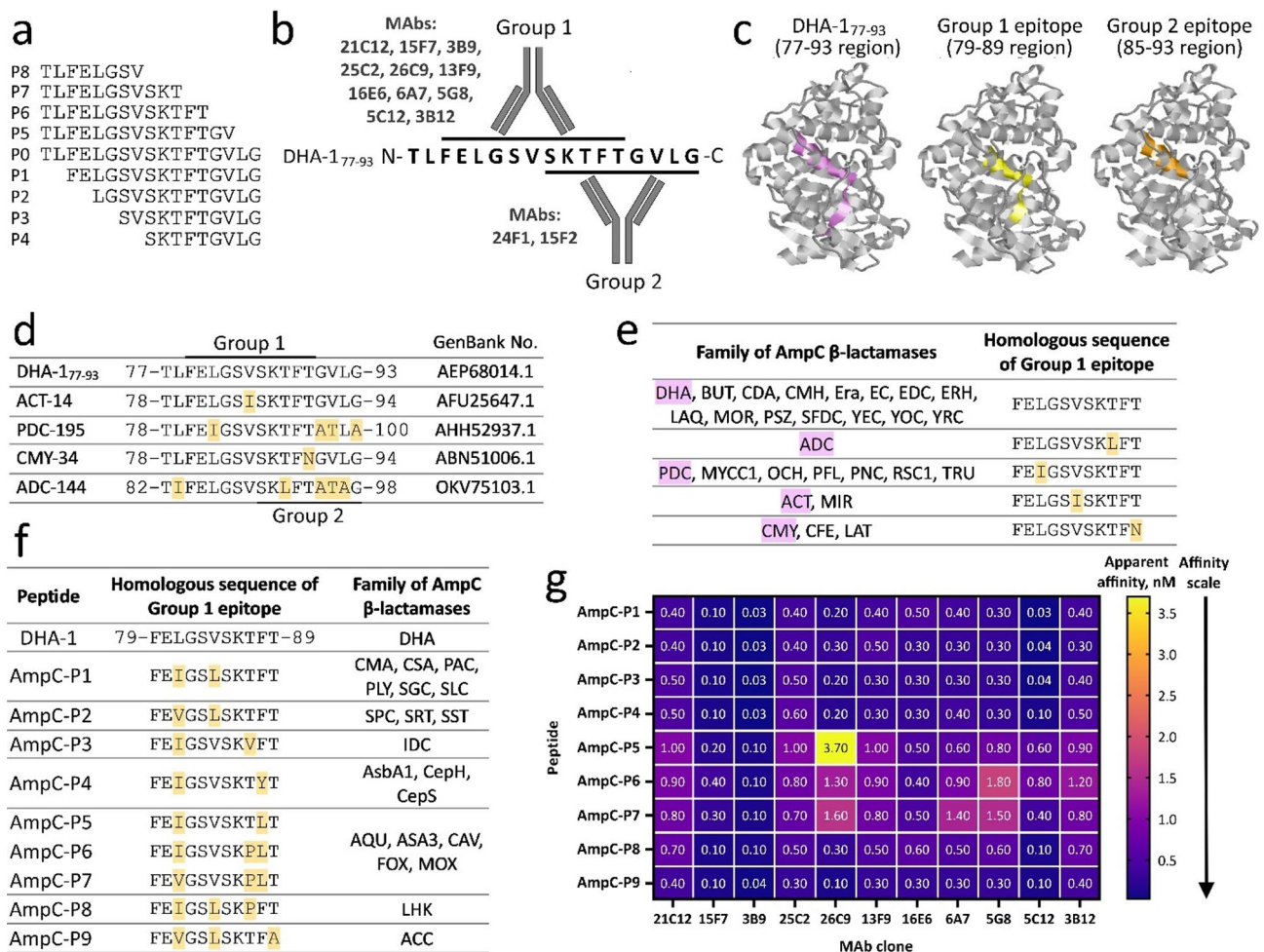


**Fig. 3.** Determined epitopes of the MABs against DHA-1<sub>77-93</sub> and the results of cross-reactivity testing. **(a)** Representation of synthetic peptides (P0–P1) used for fine mapping of MAB epitopes. P0 peptide corresponds to DHA-1<sub>77-93</sub> aa sequence. **(b)** Schematic representation of MAB recognition sites within DHA-1<sub>77-93</sub>. Based on the determined recognition sites, two groups of MABs (Group 1 and Group 2) are identified. The epitope recognised by Group 1 MABs is marked with an upper line. The epitope of Group 2 MABs is underlined. **(c)** Visualisation of the determined MAB epitopes in the DHA-1 protein. DHA-1<sub>77-93</sub>, corresponding to the 77–93 aa region in the DHA-1 protein, is coloured violet, the epitope of Group 1 MABs (79–89 aa region) is coloured yellow, and the epitope of Group 2 MABs (85–93 aa region) is marked in orange. The image of the DHA-1 protein (23–379 aa) without a signal sequence (AlphaFold Protein Structure Database, No. AF-G5DDZ0-F1-v4) is shown. **(d)** Alignment of aa sequences of DHA-1<sub>77-93</sub> and homologous regions of β-lactamases used for MAB characterisation. The positions of mismatched aa are highlighted in yellow. **(e)** Alignment of the 79–89 aa region of DHA-1, recognised by Group 1 MABs, with homologous regions of ADC, PDC, ACT, CMY (highlighted in purple) and other families of AmpC β-lactamases sharing the same region. The differences in the aa sequences are coloured yellow. **(f)** Synthetic peptides (AmpC-P1–AmpC-P9) used for MAB cross-reactivity testing and their alignment with the 79–89 aa recognition site of Group 1 MABs. The mismatched aa are coloured yellow. Each peptide corresponds to a group of AmpC β-lactamases sharing the same homologous region. **(g)** The reactivity of Group 1 MABs with synthetic peptides (AmpC-P1–AmpC-P9) tested by ELISA. The results are presented as apparent affinity values (nM).

indirect ELISA was performed using synthetic peptides (AmpC-P1–AmpC-P2) corresponding to homologous sequences of various AmpC families (Fig. 3f, g).

ELISA revealed the reactivity of Group 1 MABs with all tested peptides (Fig. 3g). The determined apparent affinity values of interactions with peptides corresponding to various AmpC families (except peptides AmpC-P5, AmpC-P6 and AmpC-P7) ranged from 0.03 to 0.1 nM, indicating high-affinity binding. Meanwhile, the apparent affinity values of MABs 26C9, 6A7, 5G8 and 3B12 with the AmpC-P5, AmpC-P6 and AmpC-P7 peptides were notably greater, ranging from 0.6 to 3.7 nM, suggesting a lower affinity to peptides corresponding to the AQU, ASA3, CAV, FOX and MOX β-lactamase families (Fig. 3f, g).

The results of MAB characterisation suggest that Group 1 MABs have similar reactivity characteristics with all tested β-lactamases. To ensure a comprehensive analysis, three MABs, 26C9, 5C12 and 21C12, representing

MAB clone	Identified MAB recognition site in DHA-1 <sup>a</sup>	MAB reactivity with peptides spanning DHA-1 <sub>77-93</sub> <sup>b</sup>										MAB grouping by determined epitopes
		P0	P1	P2	P3	P4	P5	P6	P7	P8		
21C12	79–89 aa	+	+	+			+	+	+			Group 1
15F7		+	+	+			+	+	+			
3B9		+	+	+			+	+	+			
25C2		+	+	+			+	+	+			
26C9		+	+	+			+	+	+			
13F9		+	+	+			+	+	+			
16E6		+	+	+			+	+	+			
6A7		+	+	+			+	+	+			
5G8		+	+	+			+	+	+			
5C12		+	+	+			+	+	+			
3B12		+	+	+			+	+	+			
24F1	85–93 aa	+	+	+	+	+	+				Group 2	
15F2		+	+	+	+	+	+					

**Table 2.** MAB epitope mapping with overlapping peptides spanning the DHA-1<sub>77-93</sub> sequence. <sup>a</sup>According to the full-length DHA-1 protein sequence: GenBank no. AEP68014.1. <sup>b</sup>Determined positive reaction (+) in ELISA.

different IgG subtypes (IgG1, IgG2 and IgG3, respectively), were selected for further investigation. The selection was driven by the similar reactivity profiles of the MABs combined with their distinct isotype properties, which may influence functionality and interactions. The kinetics of their interaction with one of the AmpC  $\beta$ -lactamases, rCMY-34, was analysed using total internal reflection ellipsometry (TIRE). To calculate the rate and affinity constants, a two-step kinetic binding model was applied to the experimentally obtained kinetics of the MAB and rCMY-34 interaction (Fig. 4, a). The model takes into account the formation of an intermediate immune complex<sup>20</sup>. The calculated rate and affinity constants are presented in Supplementary information file 2, Table S1. The observed affinity constants ( $K_d$ ) for MABs 26C9, 5C12 and 21C12 were in the nanomolar range and reached 5.51, 2.98 and 1.7 nM, respectively (Supplementary information file 2, Table S1), confirming the results obtained by indirect ELISA (Table 1), that all selected antibodies have high affinity to rCMY-34. The same conclusions can be drawn from the high equilibrium association constant ( $K_a$ ) values ( $1.25 \cdot 10^4$ – $4.32 \cdot 10^4$  M<sup>-1</sup> s<sup>-1</sup>) (Supplementary information file 2, Table S1).

To further characterise the selected MABs 26C9, 5C12 and 21C12, their sensitivity in detecting both recombinant and natural CMY-34 in *C. portucalensis* lysate, was evaluated by WB. rCMY-34 and lysate proteins at different concentrations were fractionated by SDS-PAGE and transferred onto a membrane. For sensitivity assessment, the detection limit was determined as the concentration of protein or lysate at which a visible band was formed. The results revealed that MAB 26C9 detected 6.25 ng, MAB 5C12 – 1.6 ng and MAB 21C12 – 12.5 ng of rCMY-34 (Supplementary information file 2, Fig. S11). Additionally, all MABs were reactive with natural CMY-34, as determined by analysing 78 ng of *C. portucalensis* lysate proteins in WB (Supplementary information file 2, Fig. S11).

Clonal differences among selected Group 1 MABs 26C9, 5C12 and 21C12 were confirmed by sequencing the variable regions of the heavy (VH) and light (VL) chains, as described previously<sup>21</sup>. VH and VL coding sequences were amplified from hybridoma genetic material with a set of previously described primers<sup>22</sup> which are specific to the variable regions of mouse immunoglobulins. Analysis of variable region sequences revealed 1–3 aa differences in the complementarity-determining regions (CDRs) 1 and 3 of the VH domain and 1–2 aa differences in the CDR-1 and CDR-3 of the VL domain. CDR-2 was identical among the analysed MABs. When CDRs of Group 1 MABs were compared with CDR regions of Group 2 MAB 15F2, no sequence similarities were identified.

Group I MABs were further *in silico* characterised by evaluating their potential reactivity with class C  $\beta$ -lactamase families or their allelic variants previously not tested experimentally. The analysis was carried out using a set of peptides corresponding to different AmpC families or their allelic variants (Fig. 4b). In total, 17 regions of  $\beta$ -lactamases from different AmpC families corresponding to the Group 1 MAB epitope were selected for further analysis (Fig. 4b). The sequences of the experimentally tested synthetic peptides were found to be highly similar, with a few exceptions towards the C-terminus of the peptides (Supplementary information file 2, Fig. S13). Similarly, untested  $\beta$ -lactamase peptides were highly similar to experimentally tested peptides (Fig. 4b; Supplementary information file 2, Fig. S13). To assess whether these peptides might also interact with Group 1 MABs, structure modelling was performed using the sequences of untested peptides and VH and VL chain sequences of MAB 21C12. The modelling was carried out following the ideas of AlphaFold-based prediction of possible protein interactions<sup>23,24</sup> and using massive sampling protocol to overcome limitations of AlphaFold in modelling antibody-antigen interactions<sup>25–27</sup>. In total, 6,000 models were generated for each  $\beta$ -lactamase peptide using AlphaFold-Multimer<sup>25–27</sup>. In most cases, selected top models of the peptide-MAB interactions had high AlphaFold accuracy self-estimation scores (Supplementary information file 2, Table S2, Fig. S14). These top models were very similar, and binding orientation of the peptides was the same as that of the DHA-1 peptide

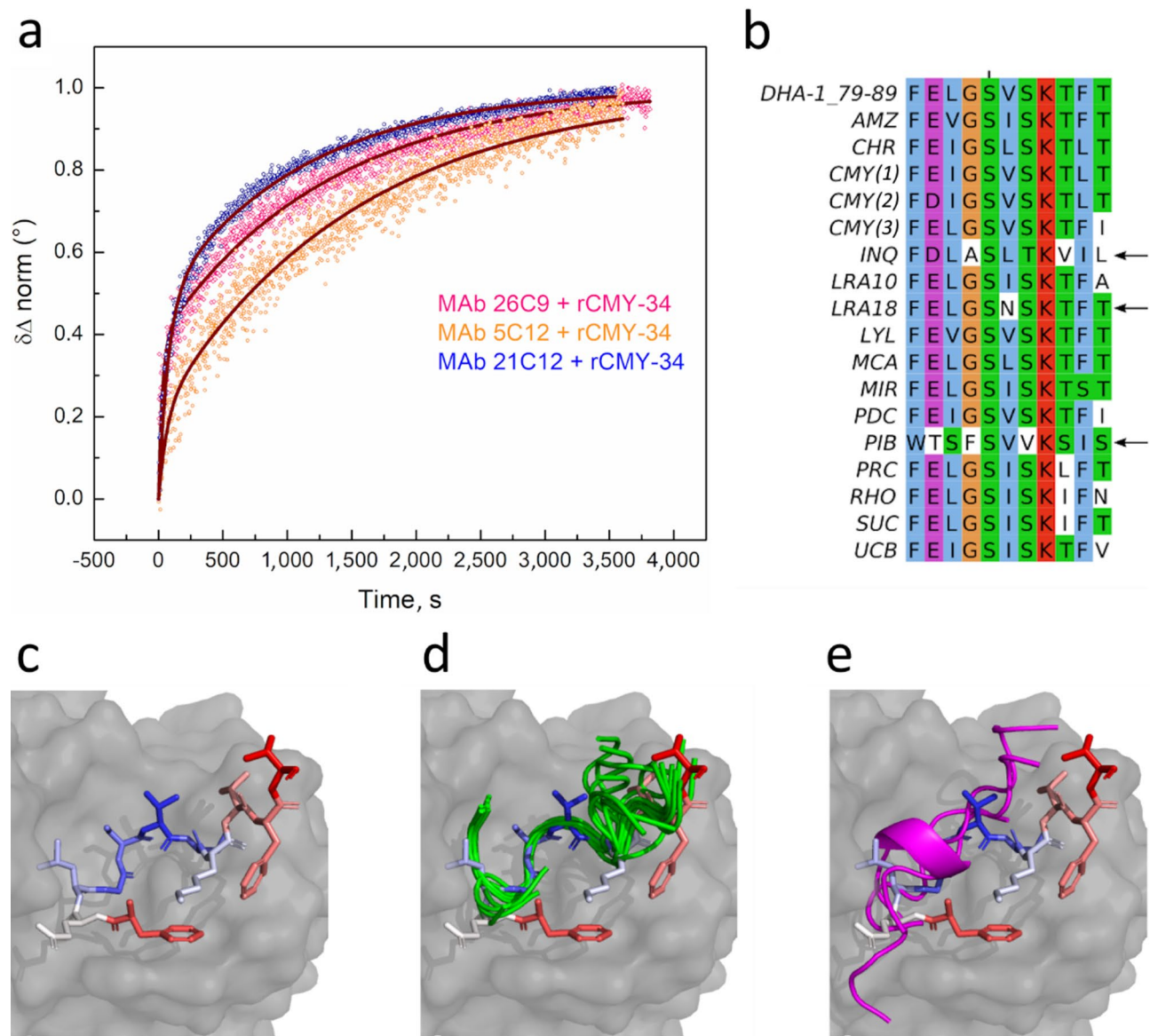


**Fig. 4.** Results of Group 1 MAb characterisation. **(a)** Normalised  $\delta\Delta$  kinetics fitted by a two-step kinetic binding model for MAb 26C9, 5C12 and 21C12 binding to rCMY-34. The scattered curves correspond to the experimental data, and the solid lines correspond to the model. **(b)** Multiple sequence alignment of the experimentally untested peptides corresponding to various families of AmpC  $\beta$ -lactamases, and DHA-1 peptide (79–89 aa) corresponding to Group 1 MAb epitope. The aa residues are coloured according to the Clustal X colour scheme. Peptides that demonstrated unreliable binding to MAb 21C12 in computational modelling are indicated with arrows. **(c)** DHA-1 peptide (79–89 aa) binding to the MAb 21C12 VH and VL domains, as predicted by AlphaFold (the antibody is shown as a gray surface, and the peptide is coloured according to the AlphaFold pLDDT values: solid red represents pLDDT < 50 (unreliable prediction), solid blue represents pLDDT > 90 (reliable prediction), light colours and white correspond to pLDDT values between these numbers). **(d)** Prediction of experimentally untested peptides binding to the MAb 21C12. Reliably predicted peptides (green) are bound in the same orientation as the DHA-1 peptide, and peptides predicted with low reliability (magenta) **(e)** have different binding orientations.

(79–89 aa), which corresponds to the Group 1 MAb epitope (Fig. 4c, d). Differences were observed mostly in the C-terminal region of the peptides. Among the experimentally tested peptides, small changes in the C-terminus did not eliminate binding to the antibody (Supplementary information file 2, Fig. S13). The modelling was unsuccessful for a few peptides, such as LRA18, INQ, and PIB, for which AlphaFold-Multimer failed to produce reliable peptide-MAb interaction models (Fig. 4e; Supplementary information file 2, Table S2, Fig. S14). Thus, structure modelling suggests that the interaction between MAbs and LRA18, INQ and PIB is unlikely. As shown by the sequence alignment (Fig. 4b, indicated with arrows), these peptides have different sequences compared to other  $\beta$ -lactamase-derived peptides. For example, the peptide corresponding to the LRA18 has a hydrophilic

asparagine (N) at the 6<sup>th</sup> position, whereas all the other peptides have bulky hydrophobic residues, such as valine (V), leucine (L) or isoleucine (I). The INQ and PIB corresponding peptides are even more different. These *in silico* generated results demonstrates the potential reactivity of the MAb 21C12 with corresponding peptides in analysed AmpC  $\beta$ -lactamases.

## Discussion

The widespread use of antibiotics in healthcare facilities and animal farming is associated with the emergence and spread of bacterial resistance mechanisms in the environment. Medical settings, wastewater treatment plants, farms and agricultural sites are the main sources of antibiotic resistance genes and antibiotic-resistant bacteria<sup>28,29</sup>. The Antimicrobial Resistance Surveillance in Europe 2023 report highlights the need for greater efforts and investments to enhance the quality, quantity and comparability of antimicrobial resistance (AMR) surveillance data. Currently observed AMR patterns, such as increasing levels of carbapenem-resistant *Acinetobacter* spp. isolates that are difficult to eradicate once they become endemic, demonstrate the need for greater efforts in the prevention and detection of antibiotic resistance<sup>30</sup>. According to the report, AMR surveillance plays an important role in the resilience and preparedness of the health system. However, the comprehensive programs and interventions still do not receive efficient support or robust funding for prevention and control of antimicrobial stewardship and surveillance<sup>30,31</sup>.

$\beta$ -lactamases are ancient and widespread enzymes in bacteria that contribute to resistance against naturally occurring  $\beta$ -lactam compounds in the environment. Ecologically,  $\beta$ -lactamases help to shape bacterial communities and facilitate the transfer of resistance genes, impacting both ecosystems and human health<sup>32,33</sup>. The production of  $\beta$ -lactamases is the most common resistance mechanism to  $\beta$ -lactam antibiotics in gram-negative bacteria. The World Health Organisation (WHO) and Centre for Disease Control and Prevention (CDC) have identified  $\beta$ -lactamase-producing gram-negative bacteria as an emerging global threat to human health<sup>34,35</sup>. The profile of resistance mechanisms may vary depending on geographical location, nevertheless, the rapid spread of new resistance mechanisms to other areas and continents remains a serious threat<sup>36</sup>. For example, the gene *bla*<sub>NDM-1</sub> encoding most  $\beta$ -lactamase-hydrolysing NDM-1  $\beta$ -lactamase, was identified in 2006, when its spread was initially limited to India<sup>37–39</sup>. However, due to the migration of infected or colonised individuals to other geographic continents, NDM-1 coding gene has spread globally within less than five years after its identification<sup>40</sup>. This example demonstrates the importance of monitoring the emergence of antibiotic resistance mechanisms, such as  $\beta$ -lactamase production, in time and tracking their geographical distribution<sup>36</sup>. Thus, identification of antibiotic resistance profiles in different geographical regions or countries can help to predict emerging resistance threats, evaluate the effectiveness of antimicrobial stewardship, guide the selection of appropriate antibiotics, and develop new treatment strategies<sup>41</sup>.

The prevalence of AmpC-mediated resistance to  $\beta$ -lactams is barely investigated globally because of the lack of surveillance and epidemiology studies on AmpC producers and the difficulties faced by microbiology laboratories in identifying this resistance mechanism in clinical isolates<sup>42</sup>. In addition, one bacterial isolate can produce multiple  $\beta$ -lactamases, such as multiple AmpC and extended-spectrum  $\beta$ -lactamase (ESBL) combinations, which cause difficulties in phenotypic identification of AmpC determinants<sup>43</sup>. According to the Beta-Lactamase Database, 61 families of class C  $\beta$ -lactamases have been identified, including more than 4,000  $\beta$ -lactamase allelic variants<sup>5</sup>. The increasing variety of AmpC causes difficulties in monitoring these enzymes because of a lack of efficient detection tools. Currently, there are no criteria approved by the Clinical and Laboratory Standards Institute for detection of AmpC  $\beta$ -lactamases in clinical isolates<sup>44</sup>. Phenotypic and molecular methods, such as PCR, are not routinely applied for AmpC identification and prevalence analysis in microbiology laboratories<sup>7</sup>. Nevertheless, several multiplex PCR systems targeting different families of AmpC coding genes have been described. For example, Mlynarcik and colleagues designed a PCR assay for rapid detection of clinically encountered  $\beta$ -lactamase-encoding genes. In this study, 67 pairs of primers targeting 12 families of AmpC were proposed for detection<sup>45</sup>. Meanwhile, Pérez-Pérez and Hanson demonstrated a multiplex PCR system suitable for differentiation of 29 plasmid-mediated *AmpC* gene variants corresponding to the MOX, CMY, LAT, DHA, ACC, MIR, ACT and FOX families of  $\beta$ -lactamases<sup>42</sup>. This system has been widely used as the gold standard for detection of *AmpC* genes<sup>46,47</sup>. A similar improved multiplex PCR system, which targets 175 *AmpC* gene variants of the MOX, CMY, LAT, DHA, ACC, MIR, ACT and FOX families, was described later<sup>48</sup>. However, due to nonspecific amplification, this method is limited by false positive results and complexity in primer design<sup>46</sup>. In addition, the described PCR systems do not cover the majority of currently identified AmpC families or their allelic variants.

Immunoassays based on the specific recognition of  $\beta$ -lactamases could offer an alternative for laboratory testing. Several studies have described the generation of antibodies against class C  $\beta$ -lactamases and their application for immunodetection of these proteins. For instance, a sandwich ELISA system utilising rabbit polyclonal antibodies against CMY-2 has been developed, which detects CMY-2 and ACT-1 class C  $\beta$ -lactamases in bacterial isolates<sup>49</sup>. Nanobodies derived from the camelid antibodies against CMY-2 were generated and applied successfully in sandwich ELISA for detection of CMY-2-producing bacteria<sup>50</sup>. Currently, rabbit polyclonal antibodies generated against *P. aeruginosa*-derived recombinant PDC  $\beta$ -lactamase (MBS1493275, MyBioSource, USA) and *E. coli* (strain K12) EC  $\beta$ -lactamase (MBS7164145, MyBioSource, USA) for application in ELISA and WB are commercially available. However, MAbs capable of detecting a wide range of AmpC  $\beta$ -lactamases have not been described yet.

This study describes MAbs with broad reactivity to AmpC  $\beta$ -lactamases, key enzymes driving bacterial resistance to  $\beta$ -lactam antibiotics. To generate these broadly-reactive MAbs, a unique immunogen was employed on the basis of the bacteriophage-derived scaffold, displaying a highly conserved 17-aa sequence from AmpC  $\beta$ -lactamases. A previous study demonstrated that polytubes formed by the yeast-expressed tail tube protein gp39 of the bacteriophage vB\_EcoS\_NBD2 elicited an immune response against the inserted peptide of interest

in mice<sup>16</sup>. Through this research, a homologous AmpC peptide was carefully selected during multiple sequence analysis of class C  $\beta$ -lactamase families and their allelic variants. The selected 17-aa sequence had several interesting features, including a small number of substitutions among class C enzymes in this region and its localisation in the core of the class C proteins. Nevertheless, this sequence does not contain the aa residues critical for the hydrolysis of  $\beta$ -lactams and is not involved in the formation of the enzyme's active site<sup>51</sup>.

Our study applied an innovative antigen generation approach utilising bacteriophage-derived polytubes, which enabled us to increase the immunogenicity of the inserted universal  $\beta$ -lactamase peptide and allowed us to generate a collection of MAb-producing hybridomas, demonstrating broad reactivity to diverse recombinant  $\beta$ -lactamases in various assays. The generated MAbs were able to detect natural CMY-34  $\beta$ -lactamase in bacterial isolate and small amounts of  $\beta$ -lactamases in WB method. Epitope analysis revealed a conserved 11 aa region within the 17 aa-long universal peptide that may represent a robust and specific target for diagnostics. Potential broad reactivity of the MAbs was confirmed with a set of synthetic peptides that correspond to different families of class C  $\beta$ -lactamases. MAb reactivity with less common AmpC variants was predicted by computational modelling employing peptides of  $\beta$ -lactamases and determined MAb 21C12 variable domain sequences. The results suggest that MAb could recognise most of the analysed synthetic and experimentally untested peptides in most  $\beta$ -lactamases, indicating their broad reactivity features. MAb analysis with total internal reflection ellipsometry method revealed the applicability of these antibodies in immunosensing technologies. Several studies have demonstrated the use of spectroscopic ellipsometry and surface plasmon resonance-based immunosensors for bacterial sensing. These label-free optical biosensors were successfully applied for detection of *E. coli*, *Salmonella* sp. and *Campylobacter jejuni*<sup>52–55</sup>. Thus, MAbs generated in this study, coupled with their ability to recognise highly conserved epitope of AmpC  $\beta$ -lactamases, represent a valuable tool for direct detection methods, enabling rapid and precise identification of antibiotic resistance determinants in protein level. Currently, the European Committee on Antimicrobial Susceptibility Testing (EUCAST) recommends several phenotypic methods for detection of AmpC  $\beta$ -lactamases, which are based on antibiotic susceptibility testing. For example, the evaluation of bacterial susceptibility to cefoxitin, ceftazidime and/or cefotaxime combinations<sup>56</sup>. Broadly-reactive AmpC-specific MAbs could serve as an additional tool for detection of these resistance determinants. Therefore, these findings characterise the developed MAbs as a unique and highly valuable resource for improving diagnostics and monitoring antibiotic resistance profiles in clinical and environmental settings. Considering the monitoring results, appropriate recommendations for antibiotic use can be provided for healthcare, veterinary and animal farming sectors in the particular geographical regions. Nevertheless, further optimisation is required to integrate the MAbs described in this study into diagnostic platforms and ensure their efficient application.

## Methods

### Cloning and expression of the chimeric gp39m\_linker\_DHA protein

The DNA sequence encoding a 17 aa-long fragment (encompassing residues 77–92) of the DHA-1 protein (GenBank no. AEP68014.1) was synthesised by oligonucleotide hybridisation. Specifically, the primers DHA\_SmaI\_F and DHA\_BamHI\_R, which contain SmaI and BamHI restriction sites (Supplementary information file 2, Table S3), respectively, were synthesised by Invitrogen. The primers were phosphorylated and inserted into the yeast expression vector pFX7\_NBD2\_gp39m\_linker, which was constructed previously<sup>15</sup>. Before ligation, vector was linearised with SmaI and BamHI (Thermo Scientific, FD0663, FD0054). The resulting construct was transformed into *E. coli* DH5 $\alpha$  (Thermo Scientific, 18265017) and verified by sequencing. The synthesis of chimeric protein was subsequently carried out in the *S. cerevisiae* AH22-214 strain (*a*, *leu2-3,112*, *his4-519*) obtained from the Institute of Biotechnology, Life Sciences Center, Vilnius University.

The cultivation of transformed yeast cells and chimeric protein synthesis were performed following previously described protocols<sup>15,57</sup>. Briefly, *S. cerevisiae* was grown in YEYP medium (1% yeast extract, 2% peptone, 3% galactose (w/v)) supplemented with 5 mM formaldehyde for 18–24 h at 30 °C with shaking (180–220 rpm). The synthesis of proteins was induced with 3% galactose for 18–24 h at 30 °C by shaking. Following cultivation, the cells were pelleted and used for protein purification.

### Isolation of chimeric polytubes

Isolation of the chimeric polytubes formed by gp39m\_linker\_DHA protein was performed as described previously<sup>58</sup>. Briefly, 5 g of wet yeast cell biomass was resuspended in 10 mL of disruption DB450 + Arg buffer (450 mM NaCl, 1 mM CaCl<sub>2</sub>, 0.01% (v/v) Triton X-100, 10 mM Tris-HCl, pH 7.2, 250 mM arginine, 2 mM phenylmethylsulphonyl fluoride (PMSF) and mechanically disrupted with glass beads by shaking. The supernatant was cleared by centrifugation at 9,400  $\times$  g for 15 min at 4 °C, loaded onto a 10 mL 40%/4 mL 30% (w/v) sucrose gradient in DB150 buffer (150 mM NaCl, 1 mM CaCl<sub>2</sub>, 0.01% (v/v) Triton X-100, 10 mM Tris-HCl, pH 7.2) and centrifuged at 140,000  $\times$  g for 2 h at 4 °C. Concentrated precipitates of chimeric polytubes were analysed by SDS-PAGE under reducing conditions. Depending on protein purity, the concentration step was repeated several times. The polytubes were dialysed against phosphate-buffered saline (PBS), supplemented with 50% glycerol and stored at –20 °C. Prior to each mouse immunisation, the glycerol was removed by dialysing the protein against PBS.

### Cloning and expression of recombinant $\beta$ -lactamases

Synthetic genes (Invitrogen) of DHA-1 (GenBank no. JN638038.1), ACT-14 (GenBank no. JX440354.1), PDC-195 (GenBank no. CP007147.1) and CMY-34 (GenBank no. EF394370.1), each with a BamHI restriction site at the 5'-end and XhoI site at the 3'-end, were cloned into the correspondingly hydrolysed pET28a(+) vector (Sigma-Aldrich, 69864) for the expression of N-terminally His-tagged proteins. Similarly, a synthetic gene of ADC-144 (GenBank no. NCXX01000069.1) was cloned into the pET28-MBP-TEV vector, fusing the protein

with MBP at the N-terminus of ADC-144 (rMBP-ADC-144). pET28-MBP-TEV vector was a gift from Zita Balklava and Thomas Wassmer (Addgene plasmid, 69929)<sup>59</sup>. The constructed vectors were evaluated by sequencing and transformed into *E. coli* Tuner (DE3) (Sigma-Aldrich, 70623). For expression of recombinant  $\beta$ -lactamases, an overnight culture of *E. coli* Tuner (DE3) was inoculated (dilution factor 1:100) into 1 L flasks with 200 mL of LB medium supplemented with 30  $\mu$ g/mL kanamycin. The bacterial culture was grown at 37 °C with shaking (220 rpm) until the optical density (OD) at a wavelength of 600 nm reached 0.6. Protein synthesis was induced by adding 0.2 mM isopropyl  $\beta$ -D-1-thiogalactopyranoside (IPTG) and incubating the culture for 4 h at 25 °C with continuing shaking. After induction, the cell culture was centrifuged at  $3,000 \times g$  for 15 min at 4 °C, washed with washing buffer (0.2 M NaCl, 20 mM Tris-HCl, pH 7.4) and centrifuged again. For recombinant protein purification, the cells from 3 flasks were combined and resuspended in 3–5 mL of purification buffer supplemented with 1 mM PMSE. For rDHA-1, rACT-14, rPDC-195 and rCMY-34 purification, the pelleted cells were resuspended in purification buffer I (0.15 M NaCl, 20 mM imidazole, 10 mM  $\beta$ -mercaptoethanol, 20 mM Tris-HCl, pH 7.4). For rMBP-ADC-144 purification, the cells were resuspended in purification buffer II (200 mM NaCl, 1 mM EDTA, 20 mM Tris-HCl, pH 7.4). Prepared cell suspensions were stored at –70 °C until purification.

### Purification of recombinant $\beta$ -lactamases

For rDHA-1, rACT-14, rPDC-195, rCMY-34 and rMBP-ADC-144 protein purification, frozen bacterial suspensions were thawed on ice, diluted with 5 mL of purification buffer I or II, respectively, containing 1 mM PMSE and disrupted by sonication. The supernatants were clarified by centrifugation at  $15,000 \times g$  for 20 min at 4 °C, followed by filtration through a 0.45  $\mu$ m polyvinylidene difluoride (PVDF) membrane. Filtered supernatants were additionally diluted (ratio 1:4) with purification buffer I or II. Purification was carried out with an ÄKTA start chromatography system (Cytiva, 29022094).

Proteins rDHA-1, rACT-14, rPDC-195, and rCMY-34 were purified using metal chelate affinity chromatography with a 1 mL HisTrap HP column (Cytiva, 29051021) according to the manufacturer's recommendations. Briefly, the sample was loaded onto the column equilibrated with purification buffer I. Proteins were eluted with elution buffer (0.15 M NaCl, 10 mM  $\beta$ -mercaptoethanol, 20 mM Tris-HCl, pH 7.4) containing an imidazole gradient (ranging from 80 to 500 mM). Eluted fractions were analysed by SDS-PAGE under reducing conditions. Fractions with the highest purity were pooled and transferred to the storage buffer (0.2 M NaCl, 20 mM Tris-HCl, pH 7.4, 2 mM dithiothreitol (DTT)). Purified proteins were aliquoted and stored at –70 °C.

Protein rMBP-ADC-144 was purified by affinity chromatography using an MBPTrap HP column (Cytiva, 29048641) according to the manufacturer's guidelines. The sample was loaded onto the column equilibrated with purification buffer II. MBP-tagged protein was eluted with purification buffer II containing 10 mM maltose. Eluted fractions were analysed and pooled as described above. Selected fractions in elution buffer were aliquoted and stored at –70 °C.

### Generation of MAbs

For generation of MAbs, 3 female BALB/c mice (6–8 weeks) were immunised subcutaneously with 50  $\mu$ g of the chimeric gp39m\_linker\_DHA protein 4 times, according to the previously described protocol<sup>60</sup>. Briefly, for the initial immunisation, the antigen was mixed with complete Freund's adjuvant. For the second injection, incomplete Freund's adjuvant was used, while subsequent immunisations were carried out by mixing the antigen with PBS. The titre of antigen-specific IgG in mouse blood was evaluated using an indirect ELISA. The mouse producing the highest titre of antigen-specific IgG received an additional boost with 50  $\mu$ g of antigen in PBS 3 days prior to hybridisation. The hybridisation procedure was carried out as described previously<sup>61</sup>. Briefly, spleen cells from the immunised mouse were fused with mouse myeloma Sp2/0 cells (ATCC, CRL-1581) using polyethylene glycol solution (Sigma-Aldrich, P7306). After fusion, the cells were cultured in Dulbecco's modified Eagle's medium (DMEM) supplemented with 15% foetal bovine serum (FBS) and a mixture of hypoxanthine, aminopterin and thymidine (HAT; Sigma-Aldrich, H0262). To select hybridomas producing antigen-specific MAbs, cell culture supernatants were screened using an indirect ELISA. Selected hybridomas were cloned by the limiting dilution method, and the clones producing antigen-specific antibodies were cryopreserved.

Animal care and experimental protocols were adhered to the ARRIVE and FELASA guidelines in accordance with Lithuanian and European legislation. BALB/c mice were obtained from Institute of Biochemistry, Life Sciences Center, Vilnius University (Vilnius, Lithuania), which has State Food and Veterinary Agency (Vilnius, Lithuania) permission to breed and use experimental animals for scientific purposes (Vet. Approval No. LT 59–13–001, LT 60–13–001, LT 61–13–004). Ethical approval was granted by State Food and Veterinary Agency (Vilnius, Lithuania), permission No. G2–117, issued 11 June 2019. The immunised mice were sacrificed by cervical dislocation (without anaesthesia) according to the requirements specified in ANNEX IV of DIRECTIVE 2010/63/EU. The death of the mice was confirmed by the onset of *rigor mortis*.

### Purification of MAbs

Generated MAbs were purified from the hybridoma cell culture supernatants using an ÄKTA start chromatographic system (Cytiva, 29022094) and a 1 mL HiTrap Protein A HP column (Cytiva, 29048576) according to the manufacturer's recommendations. Briefly, the column was equilibrated with a binding buffer (3 M NaCl, 1.5 M glycine, pH 8.9, for IgG1 purification; 0.1 M Tris-HCl, pH 8, for IgG2a and IgG3 purification). Cell culture supernatant was diluted with binding buffer (ratio 1:2 for IgG1 purification and 1:9 for IgG2a or IgG3 purification) and loaded onto the column. Antibody elution was carried out with elution buffer (100 mM glycine, pH 3), fractions containing purified antibodies were pooled, and the buffer was exchanged to PBS. Purified IgG1 and IgG2a MAbs were filtered through a 0.2  $\mu$ m filter and stored at 4 °C. After dialysis, formed

insoluble IgG3 aggregates were removed by centrifugation at  $15,000 \times g$  for 10 min. The concentration of soluble IgG3 MAbs was adjusted to 0.5–1 mg/mL, then MAbs were filtered through a 0.2  $\mu\text{m}$  filter and stored at 4 °C.

### Enzyme-linked immunosorbent assay (ELISA)

Antibody reactivity with recombinant  $\beta$ -lactamases and chimeric protein was assessed by indirect ELISA. 96-well plates (Nerbe Plus, 10-121-0000) were coated with antigen at a concentration of 3–5  $\mu\text{g}/\text{mL}$  in coating buffer (50 mM sodium carbonate, pH 9.5), 50  $\mu\text{L}$  per well, for 16 h at 4 °C. The wells were blocked with 250  $\mu\text{L}$  of 2% bovine serum albumin (BSA) (w/v) in PBS per well for 1 h at room temperature (RT). The plates were then washed twice with PBS containing 0.1% Tween-20 (v/v) (PBST) and incubated with 50–100  $\mu\text{L}$  per well of antibody sample in PBST: mouse blood (dilution range 1:300–1:38,400), undiluted hybridoma cell supernatant or purified MAbs at concentrations ranging from 66.7 to 0.0003 nM (for determination of the apparent affinities). The plates were incubated for 1 h at RT, washed 5 times with PBST, and then incubated with 50  $\mu\text{L}$  per well of horseradish peroxidase (HRP)-conjugated goat anti-mouse IgG antibody (dilution factor 1:5,000) (Bio-Rad, 1721011) in PBST for 1 h at RT. After incubation, the plates were washed 6 times with PBST. Complexes were detected by adding 50  $\mu\text{L}$  of 3,30,5,50-tetramethylbenzidine (TMB, Clinical Science Products, 01016-1-1000) to each well. The reaction was stopped by adding 25  $\mu\text{L}$  of 1 N  $\text{H}_2\text{SO}_4$  per well. The OD was measured using microplate spectrophotometer and calculated as the difference between the OD values at 450 and 620 nm (reference wavelength).

Apparent affinity values for the purified MAbs were determined from their titration curves, where the value corresponds to the MAb concentration (nM) at which the OD decreases by 50%.

HRP-conjugated MAbs were tested using a direct ELISA format. Coating, blocking, washing and other procedures were performed as described above. HRP-conjugated MAbs were serially diluted in the range of 1:50–1:36,450 (50  $\mu\text{L}$  per well).

The isotypes of the MAbs were determined using a BD Pharmingen Mouse Immunoglobulin Isotyping ELISA kit (BD Biosciences, 550487), according to the manufacturer's recommendations.

Epitope mapping of the MAbs was performed using a set of overlapping synthetic peptides (P0–P8) (GenScript) (Supplementary information file 2, Table S4) spanning the 77–93 aa region of DHA-1. For testing, MaxiSorp plates (Thermo Scientific, 442404) were coated with recombinant DHA-1 at a concentration of 3  $\mu\text{g}/\text{mL}$  in coating buffer (50  $\mu\text{L}$  per well) for 16 h at 4 °C. The wells were blocked with 300  $\mu\text{L}$  of 2% BSA (w/v) in PBS per well for 1 h at RT. During the blocking step, 0.5  $\mu\text{g}/\text{mL}$  of MAb in PBST was preincubated with 5  $\mu\text{g}/\text{mL}$  of peptide for 30 min at RT. The MAb-peptide mixture was then added to the blocked wells and incubated for an additional 1 h at RT. Secondary antibody incubation and detection were carried out as described above.

For evaluation of cross-reactivity, MAbs were tested with a set of N-biotinylated synthetic peptides (AmpC-P1–AmpC-P9) (GenScript) corresponding to the 79–89 aa segment of DHA-1 and containing a linker (-SGSG-) connecting biotin to the peptide (Supplementary information file 2, Table S5). For testing, MaxiSorp plates were coated with 50  $\mu\text{L}$  per well of Pierce avidin (Thermo Scientific, 21128) at a concentration of 5  $\mu\text{g}/\text{mL}$  in deionised water for 16 h at 4 °C. The wells were blocked with 250  $\mu\text{L}$  per well of 2% BSA (w/v) in PBS for 1 h at RT, then washed and incubated with 100  $\mu\text{L}$  per well of synthetic peptides at a concentration of 10  $\mu\text{g}/\text{mL}$  in PBST for 1 h at RT. After incubation, 100  $\mu\text{L}$  per well of MAb at 5  $\mu\text{g}/\text{mL}$  in PBST was added to the washed wells and incubated for 1 h at RT. Subsequently, incubation with HRP-conjugated goat anti-mouse IgG antibodies and TMB was performed as described above.

### Mab conjugation with horseradish peroxidase (HRP)

Antibody conjugation was carried out using a periodate method as described previously<sup>62</sup>. Briefly, 5 mg of HRP (Sigma-Aldrich, 116216) was dissolved in 1 mL of distilled water, mixed with 0.25 mL of 0.2 M  $\text{NaIO}_4$  solution, and incubated for 20 min at RT with rotation in the dark. The HRP was then transferred to 1 mM sodium acetate buffer (pH 4.5) using PD-10 desalting columns prepacked with Sephadex G-24 resin (Cytiva, 17085101). Prior to conjugation, the MAbs were dialysed into 10 mM sodium carbonate buffer (pH 9.5) and then mixed with prepared HRP at 1:1 ratio (w/w). In the next step, pH of the reaction mixture was adjusted to 9.5 with 0.2 M sodium carbonate (pH 9.5), and the mixture was incubated for 2 h at RT with rotation in the dark. After incubation, 4 mg/mL  $\text{NaBH}_4$  solution was added to the final concentration of 0.2–0.4 mg/mL, and the mixture was incubated for 2 h at 4 °C in the dark. Generated conjugates were dialysed into PBS, combined with 0.1% BSA (w/v) and 50% glycerol (v/v), verified by direct ELISA and stored at  $-20$  °C.

### Western blot (WB)

WB analysis for MAb characterisation was performed as described previously<sup>63</sup>. Briefly, 0.5–1  $\mu\text{g}$  of purified protein or 7  $\mu\text{g}$  of bacterial lysate per lane was fractionated in 12% polyacrylamide gels by SDS-PAGE under reducing conditions and semidry transferred to a 0.45  $\mu\text{m}$  PVDF membrane. After transfer, the membranes were blocked with 2% milk powder (w/v) in PBS for 1 h at RT and then incubated with MAbs at a concentration of 0.5  $\mu\text{g}/\text{mL}$  in PBST with 2% milk powder (w/v) for 1 h at RT, followed by 1 h incubation with goat anti-mouse IgG-HRP detection antibodies (dilution ratio 1:4,000, Bio-Rad, 1721011). Detection was carried out using NeA-Blue Precip reagent (Clinical Science Products, 01283-1-200).

For the analysis of chimeric gp39m\_linker\_DHA, protein samples were fractionated by SDS-PAGE under reducing conditions using 14% polyacrylamide gels. WB analysis was performed as previously described<sup>15</sup> using in-house produced murine gp39-specific polyclonal antibodies<sup>16</sup> at a concentration of 2  $\mu\text{g}/\text{mL}$  in Tris-buffered saline with Tween-20 (TBS-T, 137 mM NaCl, 0.1% Tween-20 (v/v), 20 mM Tris, pH 7.6) and goat anti-mouse IgG-HRP detection antibodies in TBS-T (dilution ratio 1:3,000, BioRad, 1721011).

### Immunoprecipitation (IP)

IP was carried out using rProtein G Sepharose Fast Flow resin (Cytiva, 17127905) according to the manufacturer's guidelines. Briefly, 125  $\mu$ l of resin was washed 4 times with 0.1 M Tris-HCl (pH 8) buffer solution by centrifugation at  $12,000 \times g$  for 30 s. The equilibrated resin was blocked with ROTI Block (Carl Roth, A151.1) for 1 h at RT with rotation and then incubated with 25  $\mu$ g of MAb in 0.1 M Tris-HCl (pH 8) for 1 h at RT with rotation. After incubation, formed complexes were washed 4 times with PBST, divided into 5 separate tubes and incubated with 40  $\mu$ g per tube of bacterial lysate or 5  $\mu$ g per tube of rDHA-1 in PBST for 1.5 h at RT with rotation. After incubation, complexes were washed 4 times with PBST, and protein elution was performed with 0.1 M glycine (pH 3) buffer. Eluted fractions were mixed with reducing sample buffer, boiled for 10 min at 100 °C and fractionated in the 12% polyacrylamide gel by SDS-PAGE under reducing conditions, followed by WB analysis. For IP, in-house generated irrelevant IgG1 MAb 18E4 against the allergen Der p 23, IgG2a MAb 20G11 and IgG3 MAb 3D7 against the SARS-CoV-2 spike protein were used as isotype controls. For WB analysis, HRP-conjugated MAb 26C9 against the DHA-1<sub>77-93</sub> was used as a detection antibody (dilution ratio 1:500 with 2% milk powder (w/v) in PBST).

### Sequencing of MAb variable regions

Sequencing of the MAb heavy (VH) and light chain (VL) variable regions was carried out as described previously<sup>21</sup>. Briefly, total RNA was isolated from hybridoma cells using GeneJET RNA Purification Kit (Thermo Scientific, K0732) according to the manufacturer's instructions. In the next step, using the extracted RNA as a template, reverse transcription was performed with the RevertAid First Strand cDNA Synthesis Kit (Thermo Scientific, K1621), according to the manufacturer's guidelines, and VH and VL coding regions were amplified using previously described<sup>22</sup> primers (Supplementary information file 2, Table S6). PCR products were subsequently cloned using the CloneJET PCR Cloning Kit (Thermo Scientific, K1232) and verified by sequencing. VH and VL coding sequences were identified and analysed using IgBlast tool of the National Centre for Biotechnology Information (NCBI)<sup>64</sup>. For determination of the complementarity-determining regions (CDRs), the IMGT/V-QUEST tool (version 3.6.1) was utilised<sup>65,66</sup>.

### Total internal reflection ellipsometry (TIRE) setup for real-time kinetics measurement

For TIRE, M-2000X J.A. Woollam (Lincoln) ellipsometer with a rotating compensator, BK7 70° glass prism and gold-covered SPR sensor discs were used. Measurements were performed at 70° incident angle in the spectral wavelength range from 200 to 1,000 nm. Ellipsometric parameters  $\Psi$  and  $\Delta$  were monitored in real time, allowing to evaluate antibody-antigen interactions and calculate kinetic constants. Data analysis was carried out using Complete EASE software from J. A. Woollam Company. The determined association rate constant ( $k_a$ ) indicates the rate of the antigen-antibody binding, and a higher value indicates rapid formation of the MAb-rCMY-34 immune complex. After association, the stabilisation of the encounter complex is represented by the rate constant ( $k_r$ ). Conversely, a lower dissociation rate constant ( $k_d$ ) value specifies a lower dissociation rate at the formed intermediate complex, reflecting its persistence<sup>67</sup>.

To determine the kinetic constants of immune complex formation, TIRE measurements were performed according to a previously described protocol<sup>68</sup>. In summary, a self-assembling monolayer (SAM) of 11-mercaptoundecanoic acid (11-MUA) was formed on the SPR sensor disc. The SAM was activated by N-hydroxysuccinimide (NHS) and N-(3-dimethylaminopropyl)-N'-ethyl-carbodiimide hydrochloride (EDC) chemistry, and 20  $\mu$ M solution of protein G was injected into the measurement chamber for 30 min. Once the protein G monolayer was formed on the surface, the remaining carboxy groups were blocked with 1 M ethanolamine (pH 8), and 200 nM solution of selected MAbs in PBS was injected into the chamber. After 50–60 min, when equilibrium was reached, the chamber was washed with PBS, and a 300 nM (14  $\mu$ g/mL) solution of recombinant CMY-34 was injected for 60 min. A regeneration solution of 2 M glycine (pH 2) was used to clean and reuse the prepared surface. The glycine solution detaches MAbs from protein G, allowing a new layer of MAbs to form on the same surface. Regeneration was accomplished by injecting 2 M glycine solution into the measurement chamber for 3 min, followed by washing with PBS. The experiment continued with another MAb, and interaction with rCMY-34 was carried out.

### Transmission electron microscopy

Electron microscopy was carried out as described previously<sup>15</sup>. Briefly, samples of chimeric gp39 and gp39m-linker\_DHA proteins were diluted in PBS, and 4  $\mu$ l of the protein solution (0.2–0.5 mg/mL) was placed onto 400-mesh carbon-coated copper grids. The samples were stained with 2% (w/v) uranyl acetate solution and analysed with a Morgagni-268(D) electron microscope (FEI).

### Bacterial isolates and preparation of bacterial lysates

*C. portucalensis* isolate (3826Z08) producing the CMY-34  $\beta$ -lactamase was used for MAb reactivity testing in WB and IP. The isolate was a gift from Anette M. Hammerum and colleagues<sup>19</sup>.

For preparation of bacterial lysate, the *C. portucalensis* isolate (3826Z08) was grown in LB medium supplemented with 16  $\mu$ g/mL ceftazidime for 16 h at 37 °C. The bacterial culture was pelleted by centrifugation at  $3,000 \times g$  for 10 min at 4 °C and resuspended in PBS with 1 mM PMSF. The cells were disrupted by sonication, and the supernatant was cleared by centrifugation at  $15,000 \times g$  for 20 min at 4 °C. Total protein concentration was determined using Pierce Bradford Protein Assay (Thermo Scientific, 23200), according to the manufacturer's recommendations. The supernatant was aliquoted and stored at –70 °C.

### Cefinase test

Enzymatic activity of the purified recombinant  $\beta$ -lactamases and prepared bacterial lysates was evaluated using nitrocefin-impregnated BD BBL Cefinase  $\beta$ -lactamase detection discs (BD Biosciences, 231650), according to the manufacturer's instructions. Briefly, 2.5  $\mu$ g of recombinant protein or 5  $\mu$ g of bacterial lysate was diluted with PBS to a total volume of 20  $\mu$ L, which was then dispensed onto the disc and incubated for 1 h at RT. The results were evaluated visually.

### Structure prediction of the MAb-peptide complex

Structure modelling of the interaction between the MAb 21C12 variable domains and peptides was performed by AlphaFold-Multimer<sup>25–27</sup> using the AFsample protocol<sup>27</sup>. A total of 6,000 models were generated for each peptide-MAB interaction. The models were then evaluated using AlphaFold accuracy self-estimation scores, including confidence, mean inter-chain predicted-aligned error (PAE) values, predicted LDDT (pLDDT) values for all interaction interface residues, pLDDT values for peptide-MAB interaction residues and mean peptide pLDDT values. Interaction interface residues were defined using Voronoi tessellation implemented in the Voronota software<sup>69</sup>. The models for further analysis were selected after visual analysis of the top models based on each of these scores. Typically, these were the models with maximum or close to maximum AlphaFold confidence scores, low mean inter-chain PAE values, and high mean pLDDT values for the peptide residues. These selected models were relaxed using OpenMM<sup>70</sup> to eliminate clashes.

### Data analysis and visualisation

Graphs were generated using OriginPro 8 (OriginLab) and GraphPad Prism (Dotmatics). Alignments of aa sequences were generated with Clustal Omega<sup>71</sup> and visualised using Jalview<sup>72</sup> software. The DHA-1 protein structure was visualised with RasMol<sup>73</sup> and the structure models were visualised using PyMOL<sup>74</sup>.

### Data availability

The datasets not provided in the main text or supplementary information files are available in the MIDAS repository (<https://midas.lt:443/action/resources/660ba7d4-a7fd-40bb-b9e6-bb787ef23d32>) or from the corresponding author upon reasonable request. Undisclosed variable regions of heavy chain sequences of the MABs obtained during the current study are not publicly available due to potential commercialisation purposes but might be available from the corresponding author on reasonable request.

Received: 28 January 2025; Accepted: 28 May 2025

Published online: 30 May 2025

### References

- Barriere, S. L. Clinical, economic and societal impact of antibiotic resistance. *Expert Opin. Pharmacother.* **16**, 151–153 (2015).
- Bush, K. & Jacoby, G. A. Updated functional classification of  $\beta$ -lactamases. *Antimicrob. Agents Chemother.* **54**, 969–976 (2010).
- Ambler, R. P. The structure of  $\beta$ -lactamases. *Philosophical Trans. Royal Soc. Lond. B Biol. Sci.* **289**, 321–331 (1980).
- Jacoby, G. A. AmpC  $\beta$ -Lactamases. *Clin. Microbiol. Rev.* **22**, 161–182 (2009).
- Naas, T. et al. Beta-lactamase database (BLDB) – structure and function. *J. Enzyme Inhib. Med. Chem.* **32**, 917–919 (2017).
- Brandt, C. et al. In Silico Serine  $\beta$ -lactamases analysis reveals a huge potential resistome in environmental and pathogenic species. *Sci. Rep.* **7**, 43232 (2017).
- Tamma, P. D. et al. A primer on AmpC  $\beta$ -Lactamases: necessary knowledge for an increasingly Multidrug-resistant world. *Clin. Infect. Dis.* **69**, 1446–1455 (2019).
- Ronni Mol, P., Shanthi, G., Al-Mahmeed, A., Bindayna, K. M. & Shahid, M. Class C type  $\beta$ -lactamases (AmpC  $\beta$ -lactamases). in *Beta-Lactam Resistance in Gram-Negative Bacteria* (eds Shahid, M., Singh, A. & Sami, H.) 93–123 (Springer Nature, Singapore, doi:[https://doi.org/10.1007/978-981-16-9097-6\\_6](https://doi.org/10.1007/978-981-16-9097-6_6). (2022).
- Papp-Wallace, K. M., Mack, A. R., Taracila, M. A. & Bonomo, R. A. Resistance to novel  $\beta$ -Lactam- $\beta$ -Lactamase inhibitor combinations. *Infect. Dis. Clin. North. Am.* **34**, 773–819 (2020).
- Rodríguez-Baño, J., Gutiérrez-Gutiérrez, B., Machuca, I. & Pascual, A. Treatment of infections caused by Extended-Spectrum-Beta-Lactamase-, AmpC-, and Carbapenemase-Producing *Enterobacteriaceae*. *Clin Microbiol. Rev.* **31**, (2018).
- Kuil, A. et al. W. National laboratory-based surveillance system for antimicrobial resistance: a successful tool to support the control of antimicrobial resistance in the Netherlands. *Eurosurveillance* **22**, (2017).
- Diallo, O. O. et al. Antibiotic resistance surveillance systems: A review. *J. Glob Antimicrob. Resist.* **23**, 430–438 (2020).
- Boattini, M. et al. *Enterobacteriales* carrying chromosomal AmpC  $\beta$ -lactamases in Europe (EuESCPM): epidemiology and antimicrobial resistance burden from a cohort of 27 hospitals, 2020–2022. *Int. J. Antimicrob. Agents.* **63**, 107115 (2024).
- European Centre for Disease Prevention and Control. Antimicrobial resistance (AMR) reporting protocol 2023. (2023). [https://www.ecdc.europa.eu/sites/default/files/documents/EARS-Net-reporting-protocol-2023\\_1.pdf](https://www.ecdc.europa.eu/sites/default/files/documents/EARS-Net-reporting-protocol-2023_1.pdf)
- Špakova, A. et al. vB\_EcoS\_NBD2 bacteriophage-originated polytubes as a carrier for the presentation of foreign sequences. *Virus Res.* **290**, 198194 (2020).
- Avizhienė, A., Dalgėdienė, I. & Armalytė, J. Petraitytė-Burkeikienė, R. Immunogenicity of novel vB\_EcoS\_NBD2 bacteriophage-originated nanotubes as a carrier for peptide-based vaccines. *Virus Res.* **345**, 199370 (2024).
- Pichichero, M. E. Protein carriers of conjugate vaccines: characteristics, development and clinical trials. *Hum. Vaccin Immunother.* **9**, 2505–2523 (2013).
- Swaminathan, A., Lucas, R. M., Dear, K. & McMichael, A. J. Keyhole limpet haemocyanin – a model antigen for human immunotoxicological studies. *Br. J. Clin. Pharmacol.* **78**, 1135–1142 (2014).
- Hammerum, A. M., Lester, C. H., Jakobsen, L. & Porsbo, L. J. Faecal carriage of extended-spectrum  $\beta$ -lactamase-producing and AmpC  $\beta$ -lactamase-producing bacteria among Danish army recruits. *Clin. Microbiol. Infect.* **17**, 566–568 (2011).
- Balevicius, Z. et al. Modelling of immunosensor response: the evaluation of binding kinetics between an immobilised receptor and structurally-different genetically engineered ligands. *Sens. Actuators B Chem.* **297**, 126770 (2019).
- Stravinskiene, D., Sliziene, A., Baranauskiene, L., Petrikaite, V. & Zvirbliene, A. Inhibitory monoclonal antibodies and their Recombinant derivatives targeting Surface-Exposed carbonic anhydrase XII on Cancer cells. *Int. J. Mol. Sci.* **21**, 9411 (2020).

22. Pleckaityte, M., Mistiniene, E., Lasickiene, R., Zvirblis, G. & Zvirbliene, A. Generation of Recombinant single-chain antibodies neutralising the cytolytic activity of vaginolysin, the main virulence factor of *Gardnerella vaginalis*. *BMC Biotechnol.* **11**, 100 (2011).
23. Yu, D., Chojnowski, G., Rosenthal, M. & Kosinski, J. AlphaPulldown—a python package for protein–protein interaction screens using AlphaFold-Multimer. *Bioinformatics* **39**, (2023).
24. Bryant, P., Pozzati, G. & Elofsson, A. Improved prediction of protein-protein interactions using AlphaFold2. *Nat. Commun.* **13**, 1265 (2022).
25. Jumper, J. et al. Highly accurate protein structure prediction with alphafold. *Nature* **596**, 583–589 (2021).
26. Evans, R., O'Neill, M., Pritzel, A., Antropova, N. & Senior, A. Protein complex prediction with AlphaFold-Multimer. *bioRxiv* (2022).
27. Wallner, B. AFsample: improving multimer prediction with alphafold using massive sampling. *Bioinformatics* **39**, (2023).
28. Ding, D. et al. The spread of antibiotic resistance to humans and potential protection strategies. *Ecotoxicol. Environ. Saf.* **254**, 114734 (2023).
29. Hu, Y., Gao, G. F. & Zhu, B. The antibiotic resistome: gene flow in environments, animals and human beings. *Front. Med.* **11**, 161–168 (2017).
30. European Centre for Disease Prevention and Control and World Health Organization. Antimicrobial Resistance Surveillance in Europe 2023 – 2021 Data. (2023).
31. Laxminarayan, R. et al. The lancet infectious diseases commission on antimicrobial resistance: 6 years later. *Lancet Infect. Dis.* **20**, e51–e60 (2020).
32. Larsson, D. G. J. & Flach, C. F. Antibiotic resistance in the environment. *Nat. Rev. Microbiol.* **20**, 257–269 (2022).
33. Aminov, R. I. & Mackie, R. I. Evolution and ecology of antibiotic resistance genes. *FEMS Microbiol. Lett.* **271**, 147–161 (2007).
34. *Antibiotic Resistance Threats in the United States, 2019*. (2019). <https://doi.org/10.15620/cdc.82532>
35. World Health Organization. Prioritisation of pathogens to guide discovery, research and development of new antibiotics for drug-resistant bacterial infections, including tuberculosis. Preprint at. (2017).
36. Bush, K. & Bradford, P. A. Epidemiology of  $\beta$ -Lactamase-Producing pathogens. *Clin Microbiol. Rev* **33**, (2020).
37. Yong, D. et al. Characterisation of a new Metallo- $\beta$ -Lactamase gene, *Bla*<sub>NDM-1'</sub>, and a novel erythromycin esterase gene carried on a unique genetic structure in *Klebsiella pneumoniae* sequence type 14 from India. *Antimicrob. Agents Chemother.* **53**, 5046–5054 (2009).
38. Castanheira, M. et al. Early dissemination of NDM-1- and OXA-181-Producing *Enterobacteriaceae* in Indian hospitals: report from the SENTRY antimicrobial surveillance program, 2006–2007. *Antimicrob. Agents Chemother.* **55**, 1274–1278 (2011).
39. Kumarasamy, K. K. et al. Emergence of a new antibiotic resistance mechanism in india, pakistan, and the UK: a molecular, biological, and epidemiological study. *Lancet Infect. Dis.* **10**, 597–602 (2010).
40. Khan, A. U. & Nordmann, P. Spread of carbapenemase NDM-1 producers: the situation in India and what May be proposed. *Scand. J. Infect. Dis.* **44**, 531–535 (2012).
41. Cantón, R. et al. Antimicrobial surveillance: A 20-year history of the SMART approach to addressing global antimicrobial resistance into the future. *Int. J. Antimicrob. Agents.* **62**, 107014 (2023).
42. Pérez-Pérez, F. J. & Hanson, N. D. Detection of Plasmid-Mediated AmpC  $\beta$ -Lactamase genes in clinical isolates by using multiplex PCR. *J. Clin. Microbiol.* **40**, 2153–2162 (2002).
43. Thomson, K. Controversies about Extended-Spectrum and AmpC Beta-Lactamases. *Emerg. Infect. Dis.* **7**, 333–334 (2001).
44. Clinical and Laboratory Standards Institute. CLSI. Performance Standards for Antimicrobial Susceptibility Testing. vol. CLSI supplement M100. (2023).
45. Mlynarcik, P., Dolejska, M., Vagnerova, I., Kutilová, I. & Kolar, M. Detection of clinically important  $\beta$ -lactamases by using PCR. *FEMS Microbiol. Lett* **368**, (2021).
46. Geyer, C. N. & Hanson, N. D. Multiplex High-Resolution melting analysis as a diagnostic tool for detection of Plasmid-Mediated AmpC  $\beta$ -Lactamase genes. *J. Clin. Microbiol.* **52**, 1262–1265 (2014).
47. Dallenne, C., Da Costa, A., Decré, D., Favier, C. & Arlet, G. Development of a set of multiplex PCR assays for the detection of genes encoding important  $\beta$ -lactamases in *Enterobacteriaceae*. *J. Antimicrob. Chemother.* **65**, 490–495 (2010).
48. Zhou, Q. et al. Detection of AmpC  $\beta$ -lactamases in gram-negative bacteria. *Heliyon* **8**, e12245 (2022).
49. Hujer, A. M., Page, M. G. P., Helfand, M. S., Yeiser, B. & Bonomo, R. A. Development of a sensitive and specific Enzyme-Linked immunosorbent assay for detecting and quantifying CMY-2 and SHV  $\beta$ -Lactamases. *J. Clin. Microbiol.* **40**, 1947–1957 (2002).
50. Cawez, F. et al. Development of nanobodies as theranostic agents against CMY-2-Like class C  $\beta$ -Lactamases. *Antimicrob Agents Chemother* **67**, (2023).
51. Tooke, C. L. et al.  $\beta$ -Lactamases and  $\beta$ -Lactamase inhibitors in the 21st century. *J. Mol. Biol.* **431**, 3472–3500 (2019).
52. Zangenehzadeh, S. et al. Polarisation modulated spectroscopic ellipsometry-based surface plasmon resonance biosensor for *E. coli* K12 detection. *Sci. Rep.* **14**, 27046 (2024).
53. Wang, Y., Knoll, W. & Dostalek, J. Bacterial pathogen surface plasmon resonance biosensor advanced by long range surface plasmons and magnetic nanoparticle assays. *Anal. Chem.* **84**, 8345–8350 (2012).
54. Bokken, G. C. A. M., Corbee, R. J., Knapen, F. & Bergwerff, A. A. Immunochemical detection of *Salmonella* group B, D and E using an optical surface plasmon resonance biosensor. *FEMS Microbiol. Lett.* **222**, 75–82 (2003).
55. Masdor, N., Altintas, Z. & Tohill, I. Surface plasmon resonance immunosensor for the detection of *Campylobacter jejuni*. *Chemosensors* **5**, 16 (2017).
56. European Committee on Antimicrobial Susceptibility Testing. *EUCAST guidelines for Detection of Resistance Mechanisms and Specific Resistances of Clinical and/or Epidemiological Importance v 2.0*. (2017). [https://www.eucast.org/fileadmin/src/media/PDFs/EUCAST\\_files/Resistance\\_mechanisms/EUCAST\\_detection\\_of\\_resistance\\_mechanisms\\_170711.pdf](https://www.eucast.org/fileadmin/src/media/PDFs/EUCAST_files/Resistance_mechanisms/EUCAST_detection_of_resistance_mechanisms_170711.pdf)
57. Sasnauskas, K. et al. Yeast cells allow High-Level expression and formation of Polyomavirus-Like particles. *Biol. Chem.* **380**, 381–386 (1999).
58. Aviziūnienė, A. et al. Characterisation of a panel of Cross-Reactive hantavirus nucleocapsid Protein-Specific monoclonal antibodies. *Viruses* **15**, 532 (2023).
59. Currinn, H., Guscott, B., Balklava, Z., Rothnie, A. & Wassmer, T. APP controls the formation of PI(3,5)P(2) vesicles through its binding of the PIKfyve complex. *Cell. Mol. Life Sci.* **73**, 393–408 (2016).
60. Zvirbliene, A., Pleckaityte, M., Lasickiene, R., Kucinskaite-Kodze, I. & Zvirblis, G. Production and characterisation of monoclonal antibodies against vaginolysin: mapping of a region critical for its cytolytic activity. *Toxicol.* **56**, 19–28 (2010).
61. Köhler, G. & Milstein, C. Continuous cultures of fused cells secreting antibody of predefined specificity. *Nature* **256**, 495–497 (1975).
62. Wilson, M. B. & Nakane, P. P. Recent developments in the periodate method of conjugating horseradish peroxidase (HRPO) to antibodies. in *Immunofluorescence and Related Staining Techniques* (eds Knapp, W., Holubar, K. & Wick, G.) 215–224 (Elsevier, North Holland Biomedical, Amsterdam, (1978).
63. Kucinskaite-Kodze, I., Simanavicius, M., Dapkunas, J., Pleckaityte, M. & Zvirbliene, A. Mapping of recognition sites of monoclonal antibodies responsible for the Inhibition of Pneumolysin functional activity. *Biomolecules* **10**, 1–19 (2020).
64. Ye, J., Ma, N., Madden, T. L. & Ostell, J. M. IgBLAST: an Immunoglobulin variable domain sequence analysis tool. *Nucleic Acids Res.* **41**, W34–W40 (2013).

65. Giudicelli, V., Brochet, X., Lefranc, M. P. & IMGT/V-QUEST IMGT Standardised Analysis of the Immunoglobulin (IG) and T Cell Receptor (TR) Nucleotide Sequences. *Cold Spring Harb Protoc* [pdb.prot5633](https://doi.org/10.1101/2011.01.01.100000) (2011). (2011).
66. Brochet, X., Lefranc, M. P. & Giudicelli, V. IMGT/V-QUEST: the highly customised and integrated system for IG and TR standardised V-J and V-D-J sequence analysis. *Nucleic Acids Res.* **36**, W503–W508 (2008).
67. Plikusiene, I. et al. Revealing the SARS-CoV-2 Spike protein and specific antibody immune complex formation mechanism for precise evaluation of antibody affinity. *Int J. Mol. Sci.* **24**, (2023).
68. Plikusiene, I. et al. Evaluation of affinity sensor response kinetics towards dimeric ligands linked with spacers of different rigidity: immobilised Recombinant granulocyte colony-stimulating factor based synthetic receptor binding with genetically engineered dimeric analyte derivatives. *Biosens. Bioelectron.* **156**, 112112 (2020).
69. Olechnovič, K., Venclovas, Č. & Voronota A fast and reliable tool for computing the vertices of the Voronoi diagram of atomic balls. *J. Comput. Chem.* **35**, 672–681 (2014).
70. Eastman, P. et al. OpenMM 7: Rapid development of high performance algorithms for molecular dynamics. *PLoS Comput Biol* **13**, e1005659 (2017).
71. Madeira, F. et al. The EMBL-EBI job dispatcher sequence analysis tools framework in 2024. *Nucleic Acids Res.* **52**, W521–W525 (2024).
72. Waterhouse, A. M., Procter, J. B., Martin, D. M. A., Clamp, M. & Barton, G. J. Jalview version 2—a multiple sequence alignment editor and analysis workbench. *Bioinformatics* **25**, 1189–1191 (2009).
73. Sayle, R. RASMOL: biomolecular graphics for all. *Trends Biochem. Sci.* **20**, 374–376 (1995).
74. Schrödinger, L. & DeLano, W. PyMOL. Preprint at (2020).

## Acknowledgements

We are grateful to Vytautas Rudokas and Agnė Rimkutė from the Institute of Biotechnology, Life Sciences Centre, Vilnius University, Lithuania, for the recombinant proteins and MAb used for MAb reactivity testing. The authors would like to thank Anette M. Hammerum from the Statens Serum Institute, Denmark, for CMY-34-producing *C. portucalensis* isolate and Julija Armalytė from the Institute of Biosciences, Life Sciences Centre, Vilnius University, Lithuania, for cultivation of the isolate.

## Author contributions

K.B. and I.K.K. designed the experiments, performed MAb development, characterisation and data analysis, wrote the manuscript. R.P.B. and A.A. were responsible for construction and synthesis of the chimeric protein. J.D. performed a computational analysis of MAb-peptide interactions. I.P., S.J. and M.S. performed spectral ellipsometry experiments and analysed the data. A.Ž. proposed a scientific problem, provided funding and finalised the manuscript. All the authors read and approved the manuscript.

## Funding

This study was funded by the Agency for Science, Innovation and Technology (Grant No. 01.2.2-MI-TA-K-702-05-0003) “Novel affinity binders for immunodetection of antimicrobial resistance”.

## Competing interests

The authors declare no competing interests.

## Ethics approval

Animal maintenance and experimental procedures were performed in accordance with the ARRIVE and FELASA guidelines according to Lithuanian and European legislation. Ethical approval was granted by State Food and Veterinary Agency (Vilnius, Lithuania), permission No. G2–117, issued 11 June 2019.

## Additional information

**Supplementary Information** The online version contains supplementary material available at <https://doi.org/10.1038/s41598-025-04603-2>.

**Correspondence** and requests for materials should be addressed to K.B.

**Reprints and permissions information** is available at [www.nature.com/reprints](http://www.nature.com/reprints).

**Publisher’s note** Springer Nature remains neutral with regard to jurisdictional claims in published maps and institutional affiliations.

**Open Access** This article is licensed under a Creative Commons Attribution-NonCommercial-NoDerivatives 4.0 International License, which permits any non-commercial use, sharing, distribution and reproduction in any medium or format, as long as you give appropriate credit to the original author(s) and the source, provide a link to the Creative Commons licence, and indicate if you modified the licensed material. You do not have permission under this licence to share adapted material derived from this article or parts of it. The images or other third party material in this article are included in the article’s Creative Commons licence, unless indicated otherwise in a credit line to the material. If material is not included in the article’s Creative Commons licence and your intended use is not permitted by statutory regulation or exceeds the permitted use, you will need to obtain permission directly from the copyright holder. To view a copy of this licence, visit <http://creativecommons.org/licenses/by-nc-nd/4.0/>.

© The Author(s) 2025